Spin Vortices in Cuprate Superconductors: Fictitious Magnetic Field, Fictitious Electric Field, and Persistent Current†

Hiroyasu Koizumi‡

Institute of Materials Science, University of Tsukuba, Tsukuba, Ibaraki 305-8573, Japan

Received: November 25, 2008; Revised Manuscript Received: February 18, 2009

We theoretically investigate loop currents generated by a Berry phase that arises from spin vortices and argue that a coherent collection of them forms a supercurrent in cuprate superconductors. First, we explain enhanced Nernst signals in cuprates using a fictitious electric field that arises from flow of spin vortices with their centers at sites where lattice-distortion-clad holes (small polaronic holes) reside. Assuming the coexistence of holes in large and small polaron forms, the magnitude of the Nernst signal is shown to be proportional to density and mobility of small polarons, and expressed as $e_N = c_3 T^{-1} e^{-0.5W_p/k_B T}/(1 + (2\pi m^* k_B T)/(n_s h^2) e^{-W_p/k_B T})$, where c_3 is a constant, W_p is the small polaron formation energy, n_s is the surface density of sites, and m^* is the effective mass of the large polaron; by treating unknown parameters as fitting parameters, this formula follows the experimental temperature dependence very well. From the obtained W_p value, it is indicated that superconductivity occurs at temperatures where almost all of the holes become small polarons; thus, the conventional current generation mechanism is ineffective at temperatures around T_c; however, loop current generation by the spin Berry phase is effective. We calculate the superconducting transition temperature as an order−disorder transition temperature of the loop currents. The doped hole concentration, x, dependence of the transition temperature is obtained as $T_c = T_0 \ln x/x_0$ and agrees with experimental data, where T_0 and x_0 are treated as fitting parameters. Lastly, we briefly mention an artificial nanostructure that generates a persistent current by utilizing the spin Berry phase.

I. Introduction

Since the discovery of high-transition-temperature superconducting cuprates in 1986,[1] extensive experimental and theoretical studies have been conducted. Despite all of those efforts, a theory that accounts for all major experimental facts is still not obtained. What makes the problem very difficult is that electric conduction cannot be described by the conventional transport theory based on Bloch electrons; in this system, parent compounds are Mott insulators where an insulating behavior with antiferromagnetic spin order occurs due to strong Coulomb repulsion between electrons.[2] When holes or electrons are doped, metallic conductivity appears, and if the doping is sufficient, superconductivity is realized. The metallic conductivity here is very anomalous; for example, (1) the magnitude of a metallic conductivity much less than the so-called Ioffe−Regel−Mott limit is observed;[3] (2) local spin correlation survives;[4,5] (3) a disconnected arc-shaped "Fermi surface" is observed;[6] and (4) very large Nernst signals are observed in Nernst effect experiments.[7−9] This anomalous metallic phase occurs below the temperature T^*, and is called the "pseudogap phase" since many phenomena associated with an energy gap formation are observed. In this phase, very large Nernst signals are observed; thus, it is suggested that fluctuating superconductivity already starts in this phase.[10]

In addition to the strong Coulomb repulsion or electron correlation, hole−lattice interaction is also strong. There are a number of experimental results that indicate that holes become small polarons at low temperatures. EXAFS experiments observed Cu−O bond length fluctuations[11] that seem to arise from small polaron formation; the magnitude of the bond length fluctuations agrees with those obtained by molecular orbital cluster calculations.[12] The mid-IR peak observed in optical conductivity measurements[13] is most likely due to small polarons;[14] indeed, both Cu−O bond length fluctuation and appearance of the mid-IR peak occur below T^*.[15] It is also worth noting that very recent EXAFS measurements on $La_{1.85}Sr_{0.15}Cu_{1-x}Mn_xO_4$ (M = Mn, Ni, Co) have revealed a direct connection between local lattice distortions and superconductivity.[16]

A theory for cuprate superconductivity also has to explain the local antiferromagnetic order that persists in the pseudogap phase. An hourglass-shaped magnetic excitation spectrum that retains the antiferromagnetic spin wave excitation spectrum at high energies is observed in the inelastic neutron scattering measurement.[4,5] Currently, there are two models that explain this spectrum. One is the stripe model, where the doped holes create one-dimensional channels for electric conduction ("stripes") in the antiferromagnetic insulating background.[5] In this model, the observed magnetic excitations are explained to arise from the remaining antiferromagnetic part. The other is the spin vortex model, where spin vortices with their centers at hole-occupied sites are assumed to exist in the antiferromagnetic background.[17] The experimental results agree better with the spin vortex model since it gives a circular peak distribution in constant-energy slices of the excitation spectrum; on the other hand, the stripe model gives a rectangular one, which disagrees with the experiment. It is also noteworthy that the spin vortex model explains the Drude-like peak observed in the optical conductivity measurement.[13,18] This peak is often attributed to the coherent motion of doped holes; however, this attribution contradicts the small polaron formation that is strongly suggested by the EXAFS experiment; it also contradicts the assignment that the mid-IR peak is due to small polarons. Currently, the spin vortex model is the only one that explains all three major peaks in the

† Part of the "George C. Schatz Festschrift".

‡ E-mail: koizumi@ims.tsukuba.ac.jp.

10.1021/jp810343p CCC: $40.75
Published on Web 03/13/2009

optical conductivity[13] in a consistent manner, the Drude-like peak to spin wave excitations, the mid-IR peak to small polaron formation, and the high-energy (~1.5 eV) peak to the charge transfer between Cu and Os within a CuO cluster.

Recently, a novel electric current generation mechanism, which becomes possible in the presence of spin vortices, was proposed by the present author.[19] As explained above, it is expected that spin vortices exist in cuprates; thus, this new mechanism is applicable to them. In this mechanism, an electric current is produced by a Berry phase arising from the spin vortices (a spin Berry phase), and a macroscopic current is realized as a collection of loop currents that circulate around spin vortices.[19]

The Berry phase[20] (also known as the quantum geometric phase)[21] from a spin vortex is similar to the one first found in the $E \otimes e$ Jahn−Teller system.[22] In the $E \otimes e$ Jahn−Teller case, the atomic motion around a crossing point of the adiabatic potential surfaces is under the influence of a fictitious magnetic field;[23] in the spin vortex case, the electron motion around a center of a spin vortex is under the influence of a fictitious magnetic field. In both cases, the Berry phase arises from a requirement of the single-valuedness of wave functions. In our previous work,[19] a stable loop current roughly proportional to the gradient of the Berry phase is shown to arise around spin vortices.

In this work, we investigate the superconducting transition from the pseudogap phase. We explain it as an order−disorder transition of the loop currents arising from spin vortices. First, we consider a fictitious electric field[24] from the Berry phase. We successfully explain the temperature dependence of the observed enhanced Nernst signal[8] and the magnetization accompanying it as due to the temperature dependence of the number of loop currents and their mobility. This agreement supports the idea that loop currents exist around spin vortices; it also supports the view that doped holes are in equilibrium of small and large polarons. Superconductivity occurs below the temperature where almost all of the holes become small polarons; thus, the conventional current generation mechanism is ineffective at temperatures around T_c (T_c is the superconducting transition temperature). Only loop current generation by spin vortices are effective around T_c. In this situation, the superconducting transition may be regarded as an order−disorder (Ising-model-type) transition of loop currents; that is, the superconductivity is realized when a long-range coherence is established among loop currents. We derive the doping concentration dependence of T_c based on this view. By obtaining parameters of the order−disorder Hamiltonian from the fitting to experimental data, a good agreement between theory and experiment is achieved. Lastly, we discuss a possibility of constructing an artificial nanostructure that generates a persistent current by utilizing the Berry phase from spin vortices.

II. A Berry Phase from Spin Vortices and a Fictitious Magnetic Field

In this section, we briefly review the appearance of a Berry phase and a fictitious magnetic field that originate from spin vortices. The key ingredients are a strong Coulomb interaction that makes the half-filled system (system with the equal number of conduction electrons and lattice sites) an antiferromagnetic insulator (also called the Mott insulator)[2] and a strong hole−lattice interaction that makes doped holes small polarons.

Let us take a two-dimensional square lattice in the $x-y$ plane and consider the Hubbard model given by

$$H = -\sum_{i,j,\sigma} t_{ij} c_{i\sigma}^{\dagger} c_{j\sigma} + U \sum_{j} c_{j\uparrow}^{\dagger} c_{j\uparrow} c_{j\downarrow}^{\dagger} c_{j\downarrow} \tag{1}$$

where the first and second terms describe electron hopping and on-site Coulomb interaction, respectively. The $x-y$ plane here corresponds to the CuO_2 plane of cuprates. Transfer integrals t_{ij} are t if i and j are nearest-neighbor sites and 0 otherwise. The parameters are assumed to satisfy the condition $U \gg t$; in this situation, the ground state for a half-filled system is known to be an antiferromagnetic insulator.

When holes are doped, we assume that they become small polarons due to strong hole−lattice interaction. The hole−lattice interaction is not included in the Hamiltonian in eq 1 but is present in the total Hamiltonian for the electron−lattice system. The hopping rate of the small polarons is very small; thus, the system is in an "effectively half-filled Mott insulator (EHFMI) state"[19] where electrons are in an effectively half-filled situation in which doped holes can be treated as almost immobile vacancies. If we consider the limiting case where small polarons are immobile, the Hamiltonian in eq 1 can be used as an approximation for the total Hamiltonian; in this case, polaron-occupied sites are removed from hopping-accessible sites. We use this approximation in the following.

We further assume that spin vortices are created with their centers at hole-occupied sites. Then, current flow becomes possible in the EHFMI due to the fact that local loop currents are generated around spin vortices.[19]

In the presence of spin vortices, new electron-creation operators $a_j^{\dagger}$ and $b_j^{\dagger}$ and new electron annihilation operators a_j and b_j are convenient; the latter are related to the original electron annihilation operators $c_{j\uparrow}$ and $c_{j\downarrow}$ by

$$\begin{pmatrix} a_j \\ b_j \end{pmatrix} = \frac{e^{i\chi_j/2}}{\sqrt{2}} \begin{pmatrix} e^{i\xi_j/2} & e^{-i\xi_j/2} \\ -e^{i\xi_j/2} & e^{-i\xi_j/2} \end{pmatrix} \begin{pmatrix} c_{j\uparrow} \\ c_{j\downarrow} \end{pmatrix} \tag{2}$$

where the polarization of spin is assumed to lie in the $x-y$ plane and ξ_j is the azimuth angle of the spin at the jth site. A very important point here is that a phase factor $\exp(i\chi_j/2)$ appears in eq 2 in order to ensure the single-valuedness of the transformation matrix. It compensates for the sign change of $e^{\pm i\xi_j/2}$ when ξ is shifted by 2π; we may take $\chi = \xi$ for that purpose, but other choices are also possible. The phase $\chi/2$ is a Berry phase arising from spin vortices. We will see that different choices of χ correspond to different loop currents around spin vortices. A natural choice for χ may be a harmonic function that describes the winding number associated with it; this point will be seen later.

Using the new creation and annihilation operators, the Hamiltonian is now written as

$$H = K_a + K_b + K_{ab} + H_U \tag{3}$$

where

$$\begin{aligned} K_a &= -\sum_{k,j} t_{kj} e^{i/2(\chi_k - \chi_j)} \cos\frac{\xi_k - \xi_j}{2} a_k^{\dagger} a_j \\ K_b &= -\sum_{k,j} t_{kj} e^{i/2(\chi_k - \chi_j)} \cos\frac{\xi_k - \xi_j}{2} b_k^{\dagger} b_j \\ K_{ab} &= -i\sum_{k,j} t_{kj} e^{i/2(\chi_k - \chi_j)} \sin\frac{\xi_k - \xi_j}{2} (a_k^{\dagger} b_j + b_k^{\dagger} a_j) \end{aligned} \tag{4}$$

and

$$H_U = U\sum_j a_j^\dagger a_j b_j^\dagger b_j \tag{5}$$

The zeroth order Hamiltonian H_0 is given by

$$H_0 = K_a + K_b + H_U \tag{6}$$

The zeroth order ground state for the EHFMI is given by

$$|0\rangle = \prod_j a_j^\dagger |\mathrm{vac}\rangle \tag{7}$$

where j runs through all electron-occupied sites. In the EHFMI, a spin order exists; in the zeroth-order approximation, it is given by

$$\langle 0|S_j^x|0\rangle = \frac{\hbar}{2}\cos\xi_j \quad \langle 0|S_j^y|0\rangle = \frac{\hbar}{2}\sin\xi_j \quad \langle 0|S_j^z|0\rangle = 0 \tag{8}$$

where S_j^x, S_j^y, and S_j^z are x, y, and z components of spin operator at the jth site. An antiferromagnetic order is obtained by choosing $\xi_j - \xi_k = \pi$ for nearest-neighbor pairs $\langle i, j\rangle$.

When the spin configuration is different from that of antiferromagnetism, which we assume to occur by the spin vortex formation, a "fictitious magnetic field" arises. This point is seen as follows; effects of a magnetic field $\mathbf{B} = \nabla \times \mathbf{A}$ ($\mathbf{A}$ is an electromagnetic vector potential) can be taken into account by modifying transfer integrals as

$$t_{kj} \rightarrow t_{kj}\exp\left(\mathrm{i}\frac{q}{c\hbar}\int_j^k \mathbf{A}\cdot\mathrm{d}\mathbf{r}\right) \tag{9}$$

where c is the speed of light and q is the charge; thus, the appearance of factors $\mathrm{e}^{(\mathrm{i}/2)(\chi_k-\chi_j)} = \mathrm{e}^{(\mathrm{i}/2)\int_j^k \nabla\chi\cdot\mathrm{d}\mathbf{r}}$ in eq 4 can be interpreted such that a magnetic field ("fictitious magnetic field")

$$\mathbf{B}_{\mathrm{fic}} = \nabla \times \mathbf{A}_{\mathrm{fic}} \tag{10}$$

with the vector potential

$$\mathbf{A}_{\mathrm{fic}} = \frac{c\hbar}{2q}\nabla\chi \tag{11}$$

exists in the system.

Actually, the zeroth-order state $|0\rangle$ is currentless even if the fictitious magnetic filed exists. However, if the perturbation K_b is included, current-carrying states appear. Numerical calculations using a mean field theory indicate that the fictitious magnetic field produces current roughly given by[19]

$$\mathbf{j} = -C\hbar\nabla\chi \tag{12}$$

where C is a constant and χ is a harmonic function. Actually, the conservation of charge requires that χ be a harmonic function, that is, it satisfies $\nabla^2\chi = 0$.

In Figure 1a, an example of spin vortices embedded in an antiferromagnetic background is depicted. Each spin vortex is accompanied by a loop current. In Figure 1b and c, two different current patterns that are generated by the same spin vortex pattern are depicted; the difference is due to the use of different χ. Note that the single-value condition in the unitary transformation in eq 2 does not allow zero current states. Although each loop current is rather localized around each center of the spin vortices, a macroscopic current can be generated as a collection of loop currents if the number of loop currents is large enough; an example is depicted in Figure 1d. If spin vortices are stable, loop currents produced by them are also stable. A macroscopic current such that as given in Figure 1d can be a stable current if spin vortices are intact for a long time.

III. Fictitious Electric Field and Enhanced Nernst Signal

The time variation of a vector potential $\mathbf{A}$ is known to give rise to an electric field $\mathbf{E} = -(1/c)(\partial\mathbf{A})/(\partial t)$. Likewise, a time-dependent $\mathbf{A}_{\mathrm{fic}}$ gives rise to a fictitious electric field[24] given by

$$\mathbf{E}_{\mathrm{fic}} = -\frac{1}{c}\frac{\partial\mathbf{A}_{\mathrm{fic}}}{\partial t} = -\frac{\hbar}{2q}\nabla\dot{\chi} \tag{13}$$

This is not a true electric field, but it exerts force on electrons.

When a temperature gradient exists, a flow of small polarons occurs. Then, loop currents around them move. Consequently, χ becomes time-dependent; thus, a fictitious electric field appears according to eq 13. In the following, we will show that enhanced Nernst signals observed in the pseudogap phase of cuprates[7−9] can be explained using this fictitious electric field.

The Nernst signal is measured by an experimental setup shown in Figure 2a; a temperature gradient ∇T is created in the x-direction, and a magnetic field $\mathbf{B}$ is applied in the z-direction. The fictitious electric field $\mathbf{E}_{\mathrm{fic}}$ exerts force on electrons in the y-direction; then, a real electric field develops that balances the fictitious electric field ($\mathbf{E} = -\mathbf{E}_{\mathrm{fic}}$) by the accumulation of charges on edges as in the Hall effect case. The Nernst signal is defined as the developed electric field in the y-direction divided by the temperature gradient in the x-direction.

Let us consider a rectangular system shown in Figure 2a and derive a formula for the Nernst signal e_{N}. The system has a length L_x in the x-direction ($0 \le x \le L_x$) and a width L_y in the y direction ($0 \le y \le L_y$). Using eq 13, the y component of $\mathbf{E} = -\mathbf{E}_{\mathrm{fic}}$ at $x = (L_x/2)$ is calculated as

$$E_y = \frac{\hbar}{2qL_y}\int_0^{L_y}\mathrm{d}y\frac{\partial}{\partial y}\dot{\chi}\left(\frac{L_x}{2}, y\right) = \frac{\hbar}{2qL_y}\left[\dot{\chi}\left(\frac{L_x}{2}, L_y\right) - \dot{\chi}\left(\frac{L_x}{2}, 0\right)\right] \tag{14}$$

Diamagnetic currents arise around spin vortices given by eq 12; then, the phase change of χ by the vortex flow from $x = 0$ to L_x is given by

$$\Delta\chi = \chi(L_x/2, L_y) - \chi(L_x/2, 0) = -2\pi N_{\mathrm{m}} \tag{15}$$

where N_{m} is the number of loop currents.

We denote an average velocity of the small polaron flow by v; then, $\Delta t = L_x/v$ will be the average time for the flow from $x = 0$ to L_x. The time derivative of the phase difference is approximately given by

$$\frac{\Delta\chi}{\Delta t} = -\frac{2\pi N_{\mathrm{m}}}{L_x} \tag{16}$$

Then, substituting eq 16 and $q = -e$ into eq 14, the electric field in the y-direction is obtained as

$$E_y = \frac{h\upsilon n_m}{2e} \tag{17}$$

where n_m is the surface density of loop currents given by $n_m = N_m/L_xL_y$. Finally, the Nernst signal is obtained as

$$e_N = \frac{h\upsilon n_m}{2e|\nabla T|} \tag{18}$$

A large magnetization is also observed in the Nernst effect experiment.[8] If it is produced by loop currents around spin vortices, it should be roughly proportional to n_m. Then, the temperature dependence of M is essentially that of n_m.

In order to obtain the temperature dependence of n_m, we consider the situation where small polarons coexist with large polarons of effective mass m^*.[25] The equilibrium condition between "band-like" large polarons and localized small polarons is given by

$$\frac{x - n_m}{n_m} = \frac{2\pi m^* k_B T}{n_s h^2} e^{-W_p/k_B T} \tag{19}$$

where W_p is the polaron stabilization energy, n_s is the surface density of sites, and x is the doping concentration. Here, the lattice constant of the two-dimensional square lattice of the CuO_2 plane is taken to be the unit of distance. The magnetization M is given by $M = -\gamma d n_m$, where γ is the average magnitude of a magnetic moment for a loop current and d is the distance between nearby CuO_2 planes. Using n_m obtained from eq 19, the magnetization is given by

$$-M = c_1/(1 + c_2 T e^{-W_p/k_B T}) \tag{20}$$

where $c_1 = x\gamma d$ and $c_2 = (2\pi m^* k_B)/(n_s h^2)$. In Figure 2b, experimentally observed M and its fit by treating c_1 and c_2 as fitting parameters are depicted. It is seen that the fit follows experimental results quite well. The obtained W_p from the fit indicates that almost all of the doped holes become small polarons in the superconducting phase.

Next, we obtain a formula for e_N; from eq 18, it is proportional to a product of n_m and υ. Since υ is proportional to the mobility μ ($\upsilon = \mu|\nabla T|$), e_N should be proportional to a product of n_m and μ.

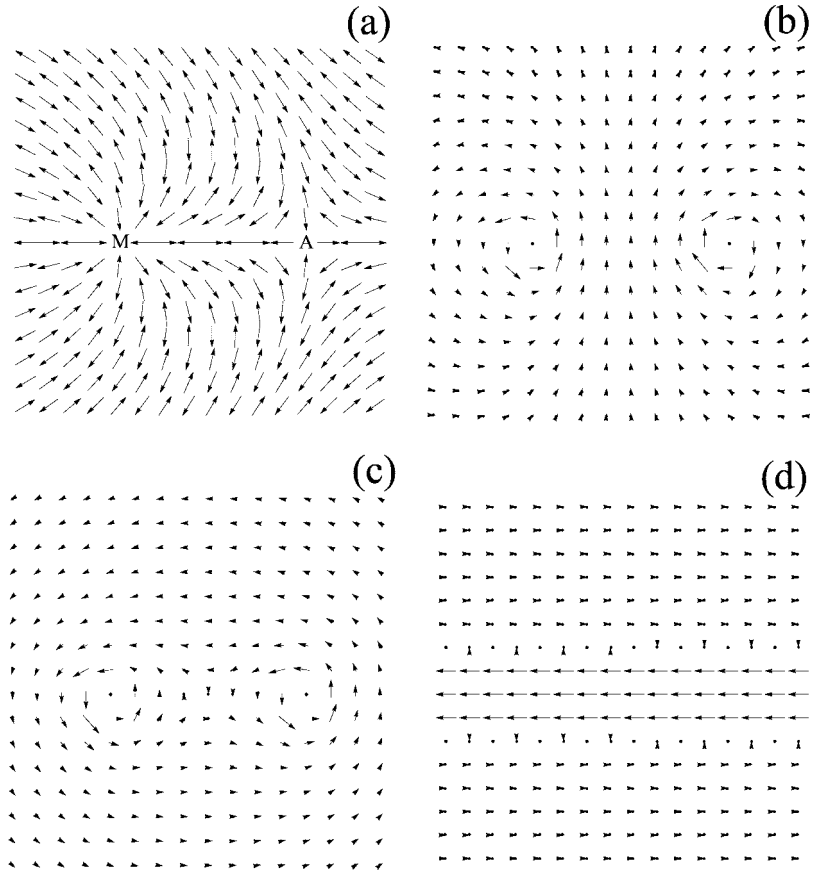

Figure 1. Spin vortices and the currents generated by them. (a) Two spin vortices embedded in the antiferromagnetic background. The spin polarization direction at the jth site in the $x-y$ plane is given by ($\cos \xi_j$, $\sin \xi_j$), where $\xi_j = \pi(j_x + j_y) + \tan^{-1}[(j_y - M_y)/(j_x - M_x)] - \tan^{-1}[(j_y - A_y)/(j_x - A_x)]$ (where (j_x, j_y) is the coordinate of the jth site and (M_x, M_y) and (A_x, A_y) are coordinates of centers of spin vortices at M and A, respectively). (b) A collection of loop currents given by $\mathbf{j} = -C\nabla\chi$, where C is a positive constant; the phase χ at the jth site is given by $\chi_j = -\tan^{-1}[(j_y - M_y)/(j_x - M_x)] + \tan^{-1}[(j_y - A_y)/(j_x - A_x)]$. (c) The same as (b) but for the current pattern produced by the phase χ given by $\chi_j = -\tan^{-1}[(j_y - M_y)/(j_x - M_x)] - \tan^{-1}[(j_y - A_y)/(j_x - A_x)]$. (d) A macroscopic current generated by a collection of loop currents; loop currents with winding number $+1$ and those with -1 are aligned in parallel lines. The definition of the winding number is given in eq 32. The total number of loop currents is 16 in the figure. Between the two lines, a directional current flow is realized with almost zero current outside.

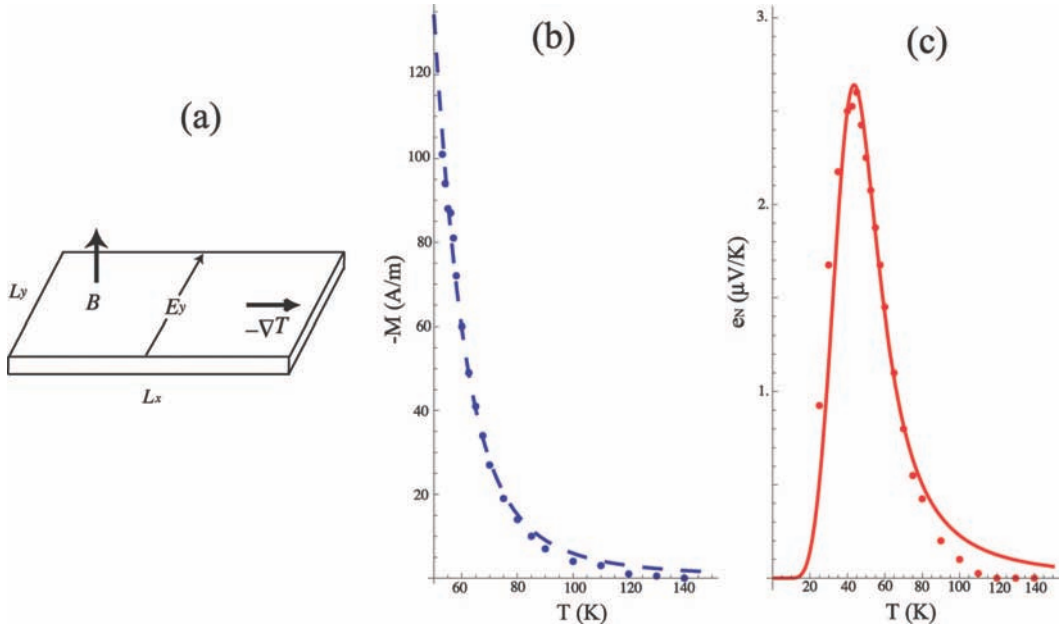

Figure 2. Experimental setup for the Nernst effect experiment and temperature dependence of magnetization M and Nernst signal e_N for the underdoped $Bi_2Sr_2CaCu_2O_{8+\delta}$ (Bi2212, $T_c = 50$ K). (a) Experimental setup. (b) Temperature dependence of M; it is fitted by eq 20 with $c_1 = 300$, $c_2 = 10$, and $W_p/k_B = 300$ K. (c) Temperature dependence of e_N; it is fitted by eq 22 with $c_3 = 5200$. Dots are experimental results.[8]

For an activation-type small polaron hopping,[2] μ is given by

$$\mu = \mu_0 T^{-1} e^{-W_H/k_B T} \tag{21}$$

where W_H is the activation energy for the polaron hopping and μ_0 is a constant. W_H may be related[2] to W_p as $W_H = 0.5W_p$, and we use this relation in the following.

Overall, the Nernst signal is expressed as

$$e_N = c_3 T^{-1} e^{-0.5W_p/k_B T}/(1 + c_2 T e^{-W_p/k_B T}) \tag{22}$$

where $c_3 = xh\mu_0/2e$ is a constant.

In Figure 2c, experimentally observed e_N and its fit by eq 22 by treating c_3 as a new fitting parameter are depicted. The fit is very good except at high temperatures. At those temperatures, the mobility given in eq 21 is probably too simple; effects of deactivation by collisions with phonons and magnons should be taken into account. However, the good agreement between the theory and experiment suggests that the above formula for e_N captures essentials of the temperature dependence of the Nernst signal. This is strong support for the existence of loop currents with their centers at small polarons in cuprates.

IV. Superconducting Transition As an Order−Disorder Transition of Loop Currents

In the previous section, the idea that loop currents exist around spin vortices is supported. It is also indicated that almost all of the doped holes become small polarons at temperatures around T_c. In this situation, a macroscopic current is possible only if it is generated by a collection of loop currents. In this section, we derive the doping concentration dependence of T_c by regarding it as an order−disorder transition of loop currents; that is, we consider that a persistent current flow becomes possible when a long-range coherence is established among loop currents generated by spin vortices.

When both a real magnetic field $\mathbf{B} = \nabla \times \mathbf{A}$ and the fictitious magnetic field $\mathbf{B}_{fic} = \nabla \times \mathbf{A}_{fic}$ exist, the electric current given in eq 12 becomes[19]

$$\mathbf{j}_e = -qC\left(\nabla\chi + \frac{2q}{\hbar c}\mathbf{A}\right) \tag{23}$$

This current is a gauge invariant as is shown below; for the gauge transformation

$$\mathbf{A}' = \mathbf{A} + \nabla f \tag{24}$$

electron operators are modified as

$$c_{j\sigma} \rightarrow c_{j\sigma} \exp\left(-i\frac{q}{\hbar c} f_j\right) \tag{25}$$

which, according to eq 2, means that χ is modified as

$$\chi'_j = \chi_j - \frac{2q}{\hbar c} f_j \tag{26}$$

Then, from eqs 24 and 26, the following sum is gauge invariant

$$\nabla\chi' + \frac{2q}{\hbar c}\mathbf{A}' = \nabla\chi + \frac{2q}{\hbar c}\mathbf{A} \tag{27}$$

Therefore, the electric current density j_e is gauge invariant.

From eq 23, the energy increase due to loop currents may be obtained as

$$U = \frac{C\hbar}{4}\int d^2 r\left(\nabla\chi + \frac{2q}{\hbar c}\mathbf{A}\right)^2 \tag{28}$$

This energy formula satisfies a required relation between U and $\mathbf{j}_e$

$$\mathbf{j}_e = -c\frac{\delta U}{\delta \mathbf{A}} \tag{29}$$

We will use this very simplified energy formula U as the Hamiltonian for the interaction among loop currents in the following.

In our previous work,[18] it is suggested that at temperatures around T_c, spin vortices are created around all doped holes. We assume this situation.

Let us consider the case where a magnetic field is absent; we may put $\mathbf{A} = 0$. Then, eq 28 is expressed as

$$U = \frac{\pi C\hbar}{2}\sum_i w_i^2 \ln\frac{R_c}{a_c} + \frac{\pi C\hbar}{2}\sum_{i\neq j} w_i w_j \ln\frac{R_c}{r_{ij}} \tag{30}$$

This formula is derived by expressing $\nabla\chi$ as a sum of loop currents

$$\nabla\chi = \sum_i \nabla\chi(i) \tag{31}$$

where $\chi(i)$ is the phase introduced to compensate the sign change caused by a single spin vortex at the ith site; w_i is the winding number for it defined by

$$w_i = \frac{1}{2\pi}\oint_{C_i} \nabla\chi(i)\cdot \mathrm{d}\mathbf{r} \tag{32}$$

where C_i is a closed path encircling the ith site. R_c and a_c are upper and lower cutoff radii of each loop current, respectively, and r_{ij} denotes the distance between the ith and jth sites.

If the magnetic field is absent, the sum of loop currents will be 0 where each loop current has the winding number $+1$ or -1. For simplicity, we only retain adjacent pairs in the second sum $\sum_{i\neq j}$ in eq 30, replace r_{ij} by its average value given by $1/(\pi x)^{1/2}$, and take a square lattice of loop currents with a lattice constant $1/(\pi x)^{1/2}$.

With the above simplifications, the following very simple interaction potential for loop currents is obtained

$$U_{\mathrm{loop}} = \frac{\pi C\hbar}{2}\ln\frac{x}{x_0}\sum_{\langle i,j\rangle} w_i w_j \tag{33}$$

where x_0 is introduced through

$$R_c = \frac{1}{\sqrt{\pi x_0}} \tag{34}$$

and the sum is taken over nearest-neighbor pairs.

The interaction potential U_{loop} is equivalent to that of an Ising model for antiferromagnets if the hole concentration satisfies $x > x_0$; two loop currents $w_i = +1$ and -1 correspond, respectively, to up and down spin states.

If T_c is identified as the order−disorder transition temperature of loop currents, it is given by

$$T_c = T_0 \ln\frac{x}{x_0} \tag{35}$$

where $T_0 = 1.14\pi C\hbar$ is a constant.

In Figure 3, the doping dependence of T_c in underdoped samples is depicted. T_0 and x_0 are obtained from the fitting to experimental data. The experimental data for La214[26] shows anomalous depression of T_c around $x = 1/8$, and the agreement is not good around there; otherwise, the fit follows the experimental data very well.

At $T = 0$ K, the insulator−superconductor transition is observed at around $x = x_0$.[3] This experimental fact is explained in the present theory, accordingly; at $T = 0$ K, the loop current generation by spin vortex formation is the only effective current generation mechanism since small polaron hopping is negligible. Therefore, if the hole density is above a critical value x_0, the electric current is a collection of loop currents, which is coherent at $T = 0$ K; thus, the system is a superconductor. However, if the hole density is less than x_0, the density of loop currents is not enough to establish a long-range coherence; thus, the system is an insulator.

If an applied magnetic field is present, a loop current pattern that is different from that for the "antiferromagnetic" loop current order mentioned above will be realized. If we denote the wave function for the "antiferromagnetic" pattern by Ψ, the wave function for a different current pattern is given by

$$\Psi' = \exp(-\mathrm{i}\sum_{k=1}^{N_e} g_k)\Psi \tag{36}$$

where N_e is the number of electrons. The phase g is given by

$$g_j = \sum_{M'} \tan^{-1}\frac{j_x - M'_x}{j_y - M'_y} - \sum_{A'} \tan^{-1}\frac{j_x - A'_x}{j_y - A'_y} \tag{37}$$

where, in the sum over M', centers of loop currents whose winding number is changed from $+1$ to -1 are included; similarly, in the sum over A', centers of loop currents whose winding number is changed from -1 to $+1$ are included. The flexible change of loop current pattern by eqs 36 and 37 may explain the very sensitive response of the supercurrent against an external magnetic field.

V. An Artificial Nanostructure That Generates a Persistent Current

In the previous section, it is expected that if a long-range coherence of a collection of loop currents generated by spin vortices is established, a macroscopic persistent current will be realized. From the fitting to experimental data, we obtain $x_0 = 0.05$. This value corresponds to $R_c = 2.5$, which suggests that if the distance between nearby holes is less than 5 times the lattice constant, interaction between loop currents is strong enough to establish coherence.

We may construct a nanostructure that generates persistent current from the above observation. An example is depicted in Figure 4, where a directional current is created between two lines of centers of loop currents. The situation here is analogous to a magnetic field produced in a solenoid; the magnetic field inside of the solenoid corresponds to the directional current,

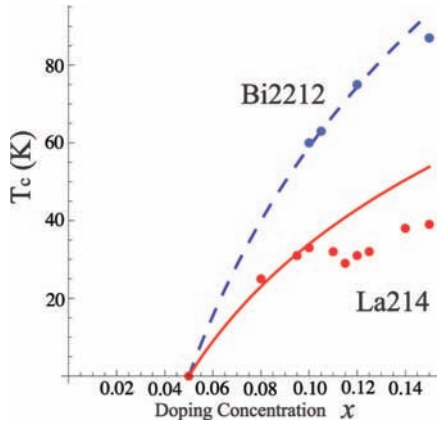

Figure 3. Doping concentration, x, dependence of the transition temperature T_c. Experimental data are fitted using eq 35 by treating x_0 and T_0 as fitting parameters; x_0 is taken to be 0.05 for all. The solid line is the result for $Bi_2Sr_2CaCu_2O_{8+\delta}$ (Bi2212) with $T_0 = 85$ K. The dashed line is the result for $La_{2-x}Sr_xCuO_4$ (La214) with $T_0 = 49$ K. The dots are experimental results.[26]

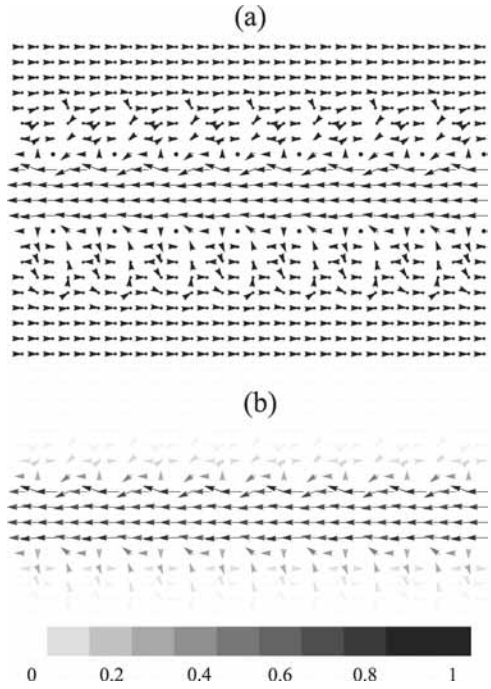

Figure 4. A macroscopic directional current generated by lines of loop currents. The centers of loop currents are marked by 16 dots in (a); the directional current flows between two lines of loop current centers. In (b), the same directional current as that given in (a) is depicted with its magnitude indicted by the gray scale.

and electric current in wires of the solenoid corresponds to vorticity of the loop currents.

In the cuprate, holes are expected to exist at each center of the loop currents; thus, if we arrange holes in this way artificially, a persistent current will be generated, even if the hole concentration is $x < 0.05$. Instead of holes, we may use some atoms (for example, Mn) as the centers of loop currents. In this way, we may obtain an enhanced stability in spin vortices. If we find a way to construct such a spin vortex structure that is similar to one given in Figure 4 and which is robust even at room temperatures, a room-temperature superconductivity may be realized.

VI. Conclusion

In the present work, we have explained enhanced Nernst signals in cuprates using a fictitious electric field that arises from the flow of spin vortices. The good agreement between the theory and experiment indicates that loop currents with their centers at small polarons exist in cuprates, and the flow of them is the origin of the enhanced Nernst signal. Using loop currents around spin vortices, we explain the superconducting transition in underdoped cuprates as an order−disorder transition of loop currents. The obtained doping concentration dependence of the transition temperature fits very well with experimental data. Thus, it is suggested that a coherent collection of loop currents generated by spin vortices is the supercurrent in cuprates. If this is the case, an artificial structure that generates a persistent current by a suitable arrangement of spin vortices will be possible.

References and Notes

(1) Bednorz, J. G.; Müller, K. A. *Z. Phys.* **1986**, *B64*, 189.
(2) Mott, N. F. *Metal-Insulator Transitions*, 2nd ed.; Taylor & Francis: London, 1990.
(3) Ando, Y.; Lavrov, A. N.; Komiya, S.; Segawa, K.; Sun, X. F. *Phys. Rev. Lett.* **2001**, *87*, 017001.
(4) Hayden, S. M.; Mook, H. A.; Dai, P.; Perring, T. G.; Doğan, F. *Nature* **2004**, *429*, 531.
(5) Tranquada, J. M.; Woo, H.; Perring, T. G.; Goka, H.; Gu, G. D.; Xu, G.; Fujita, M.; Yamada, K. *Nature* **2004**, *429*, 534.
(6) Norman, M. R.; Ding, H.; Randeria, N.; Campuzano, J. C.; Yokoya, T.; Takeuchi, T.; Takahashi, T.; Mochiku, T.; Kadowaki, K.; Guptasarma, P.; Hinks, D. G. *Nature (London)* **1998**, *392*, 157.
(7) Xu, Z. A.; Ong, N. P.; Wang, Y.; Kakeshita, T.; Uchida, S. *Nature (London)* **2002**, *406*, 257003.
(8) Wang, Y.; Li, Lu; Naughton, M. J.; Gu, G. D.; Uchida, S.; Ong, N. P. *Phys. Rev. Lett.* **2005**, *88*, 247002.
(9) Wang, Y.; Li, Lu; Ong, N. P. *Phys. Rev. B* **2006**, *73*, 024510.
(10) Emery, V. J.; Kivelson, S. A. *Nature (London)* **1995**, *374*, 434.
(11) Bianconi, A.; Saini, N. L.; Lanzara, A.; Missori, M.; Rossetti, T.; Oyanagi, H.; Yamaguchi, H.; Oka, K.; Ito, T. *Phys. Rev. Lett.* **1996**, *76*, 3412.
(12) Miyaki, S.; Makoshi, K.; Koizumi, H. *J. Phys. Soc. Jpn.* **2008**, *77*, 034702.
(13) Uchida, S.; Ido, T.; Takagi, H.; Arima, T.; Tokura, Y.; Tajima, S. *Phys. Rev. B* **1991**, *43*, 7942.
(14) Mihailovic, D.; Foster, C. M.; Voss, K.; Heeger, A. J. *Phys. Rev. B* **1990**, *42*, 7989.
(15) Oyanagi, H.; Tsukada, A.; Naito, M.; Saini, L. *Phys. Rev. B* **2007**, *75*, 024511.
(16) Zhang, C. J.; Oyanagi, H. *Phys. Rev B* **2009**, *79*, 064521.
(17) Koizumi, H. *J. Phys. Soc. Jpn.* **2008**, *77*, 104704.
(18) Koizumi, H. *J. Phys. Soc. Jpn.* **2008**, *77*, 123708.
(19) Koizumi, H. *J. Phys. Soc. Jpn.* **2008**, *77*, 034712.
(20) Berry, M. V. *Proc. R. Soc. London, Ser. A* **1984**, *392*, 45.
(21) Bohm, A.; Mostafazadeh, A.; Koizumi, H.; Niu, Q.; Zwanziger, J. *The Geometric Phase in Quantum Systems*; Springer: Berlin, Germany, 2003.
(22) Longuet-Higgins, H. C.; Öpik, U.; Pryce, M. H.; Sack, R. A. *Proc. R. Soc. London, Ser. A* **1958**, *244*, 1.
(23) Mead, C. A.; Truhlar, D. *J. Chem. Phys.* **1982**, *70*, 6090.
(24) Koizumi, H.; Takada, Y. *Phys. Rev. B* **2002**, *65*, 153104.
(25) Sumi, H. *J. Phys. Soc. Jpn.* **1972**, *33*, 327.
(26) Matsuzaki, T.; Ido, M.; Momono, N.; Dipasupil, R. M.; Nagata, T.; Sakai, A.; Oda, M. *J. Phys. Chem. Solids* **2001**, *62*, 29.

JP810343P